2007 IEEE International Conference on
Robotics and Automation
Roma, Italy, 10-14 April 2007

Tactile Imaging System for Localizing Lung Nodules during Video Assisted Thoracoscopic Surgery

Andrew P. Miller, William J. Peine, Jae S. Son, and Zane T. Hammoud M.D.

***Abstract*—Early detection and removal of small pulmonary nodules significantly improves long term survival rates for patients with lung cancer. To aid in the localization of these tumors during video assisted thoracoscopic surgery (VATS), a Tactile Imaging System (TIS) is presented. The system consists of a capacitive array sensor mounted on a minimally invasive surgical probe that is integrated with the thoracoscopic imaging. A vision-based algorithm localizes the probe in the live video and overlays a registered pseudo-color map of the measured pressure distribution on the streaming images. The surgeon can locate the hard nodules by scanning the tactile sensor head across the surface of the lung and observing the spatial variation in contact pressures caused by the elasticity differences in the underlying tissue. A validation experiment was conducted to compare the system to a current localization technique using a rigid rod. Results indicate that subjects could localize stiff lumps in lung phantoms more quickly and accurately using the TIS.**

I. Introduction

Lung cancer is the leading cause of cancer death in both men and women in the United States. According to the American Cancer Society, an estimated 163,510 deaths occurred in 2005 from the disease, accounting for 29% of all cancer related deaths in the U.S. [1]. Lung cancer has a poor prognosis, but when a tumor is discovered while still confined to the lung, five year survival rates jump from 15 to 49%. Currently, only 16% of tumors are found at an early stage [2]. Recent emphasis has therefore been placed on improving early detection [3].

Some patients with a high risk of developing lung cancer have been encouraged to get "screening" CT scans before any symptoms are evident. This has resulted in an increase in the number of solitary pulmonary nodules detected with diameters of less than 1 cm [2][3]. If a small nodule is thought to be malignant, studies indicate surgical removal is justified and the smaller the nodule at resection, the better the five year survival rate [4][5].

The surgical method used to remove a lung nodule depends on its location. Tumors found in the peripheral lung zones or on the surface of the lung can be resected using minimally invasive surgical techniques, often referred to as video-assisted thoracoscopic surgery (VATS). In these procedures, small incisions are used to gain access to the thoracic cavity. Rigid endoscopes, or thoracoscopes, are used to visualize the surgical site, and long shafted instruments allow manipulation of the tissue. VATS is preferred to a large incision, open chest thoracotomy because patient trauma, pain, length of hospital stay, and recovery time are all reduced.

This work was funded by Purdue University. A. P. Miller and W. J. Peine are with the Mechanical Engineering Department, Purdue University, West Lafayette, IN 47907 USA. J. S. Son is with Medical Tactile, Inc, Los Angeles, CA, and Z. T. Hammoud is with the Thoracic Surgery Division, Department of Surgery, Indiana University School of Medicine.

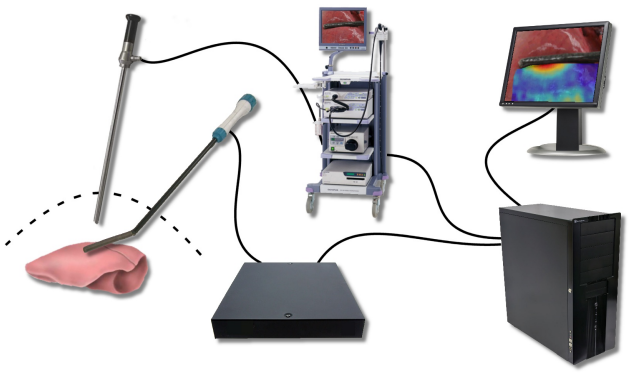

Fig. 1. Conceptual diagram of the TIS for video-assisted thoracic surgery.

During VATS, accurate localization of the embedded tumor is critical to ensure that the entire nodule is removed and to minimize the amount of healthy lung tissue resected. Unfortunately, localization using current methods is difficult because the tumors are often not visible from the lung surface [6]. Since the lung is partially deflated during the procedure, the spatial relationship of the tumor to surrounding tissues in the preoperative imaging is of minimal value. The surgeon knows which lobe and general area to search, but must actively palpate to find the exact location.

A. Current Nodule Localization Methods

Several techniques are currently used to aid the localization of tumors, but each falls short, often leading to frustration and the need for a full thoracotomy. The most basic and frequently used method is "instrument palpation" wherein a long metal rod inserted through the chest wall is slid against lung surface to "feel" for the hard inclusion in the soft lung tissue. This technique is less than ideal and can be quite time consuming – especially with deep tumors less than 2 cm in diameter. After finding the tumor with the probe, the surgeon typically inserts a single finger through the incision to palpate the area to confirm the tumor's location. If the nodule cannot be felt, VATS methods are abandoned and a thoracotomy is performed so the surgeon can directly palpate the lesion.

Other clinical localization methods exist based upon

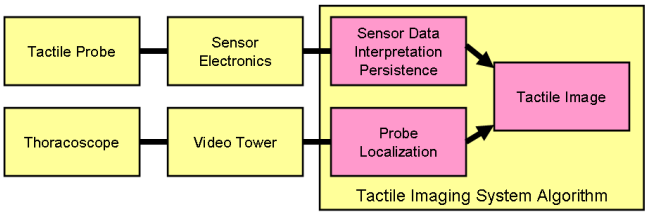

Fig. 2. System Architecture of the TIS.

various technologies. Several involve insertion of a marker (hook wire, spring, radiotracer, or dye) near the tumor immediately prior to the surgery using percutaneous needle puncture under CT guidance [7][8]. Thoracoscopic ultrasound (US) has also been explored as a means to localize tumors during VATS [9]. However, the technique is not widely used because a specialist is required to interpret the ultrasound image and the lung must be fully deflated to obtain proper images—often an impossibility in patients with obstructive diseases such as centrilobular emphysema [10].

The research community has presented several new localization techniques. Kawahara et al. developed a non-contact method using air bursts to deform tissue and then measure the resulting deformation with a laser [11]. Peine developed a tele-taction system integrated into a hand held surgical probe [12] where contact pressures measured with a tactile sensor were recreated directly on the surgeon's finger using a shape display. This method proved to be difficult to implement because of the mechanical impracticalities of individually actuating a dense array of pins.

B. *Tactile Imaging System*

This paper builds on the work of [12] and describes a new system for localization of small pulmonary nodules during VATS. Tactile sensors are integrated into a minimally invasive instrument and measure distributed pressure in a manner similar to the human finger. The Tactile Imaging System (TIS), as shown in Fig.1, will allow surgeons to explore the entire lung with the effectiveness of open incision palpation. To reduce mental workload, the tactile "map" of distributed contact pressures is overlaid directly onto the thoracoscopic video feed as a pseudo-color map. It is our expectation that the TIS will enable more procedures to be performed using minimally invasive techniques by increasing the surgeon's confidence in localization of small peripheral nodules.

C. *Paper Organization*

The major components of the Tactile Imaging System are described in detail in Section 2, with emphases on the sensor, probe mechanics, and image processing. Section 3 describes the experiment used to validate the performance of the system in a dry lab setting. Section 4 describes the results of the validation experiment and evaluates the current system. Section 5 draws conclusions about the system and describes additional applications for tactile imaging.

II. TACTILE IMAGING SYSTEM DESIGN

A. *System Architecture and Specifications*

The TIS, outlined in Fig. 2, consists of a tactile array sensor mounted on a minimally invasive surgical probe. By translating the handle on the proximal end of the instrument while using the trocar as fulcrum, the surgeon can contact and scan the pivoting sensor head across the surface of the lung to see the varying pressure distribution on the tactile array sensor surface caused by the elasticity differences of the underlying tissue. Dedicated electronics measure this pressure distribution and communicate the signals to a computer. As the sensor slides over a hard inclusion within the lung tissue, a stress concentration is created and becomes visible in the tactile data. The design specifications for the TIS are outlined in Table 1.

B. *Probe Design*

The tactile probe, shown in Fig. 3, is a modified laparoscopic fan retractor. The shaft and tip have an outer diameter of 10 mm. On the distal end, the retractor fingers have been removed and replaced by a tactile probe head. A tactile array sensor is mounted on the underside of the head. The head is manually articulated by twisting the knob at the base of the probe handle.

Table 1. TIS Design specifications

Max probe shaft diameter of 10 mm
Min probe shaft length of 30 cm
50 mm long tactile sensor mounted on 80 mm long TIS head
Tactile sensor input pressure range is 0 to 170 kPa
Total contact force on sensor head less than 14 N
Update of tactile data at video refresh rate (30 Hz) is adequate for nodule localization
Sensor head covered with layer of polyurethane or TPE
Sensor head is a uniform diameter cylinder (single curvature)
LEDs on back of sensor head can be used for localization
TIS image on secondary monitor visible from sterile field
Lung tissue and camera remain stationary enough during palpation process for tactile maps to be valid

C. *Sensor Design*

The tactile sensor in the TIS is based on capacitance based pressure array technology developed by Pressure Profile Systems, Inc (Los Angeles, CA). The sensor used in the TIS has 3 columns and 12 rows and is mounted on the underside of the probe head, opposite the arrow in Fig. 3. It is effective for pressures up to 170 kPa with 8 bits of resolution. Details of the sensor design can be found in [13].

This capacitance based sensor technology is currently being used in the SureTouch Visual Mapping System (MTI, Los Angeles, CA) for breast cancer screening and nodule characterization. The system has been FDA cleared for documenting palpable breast lesions and is currently being

sold to breast surgeons and radiologists. It has the potential for assisting breast cancer detection by providing objective, quantifiable, and repeatable results which are currently lacking in manual clinical exams. Laboratory and clinical studies have shown that the tactile sensor technology is more sensitive than the average level of manual palpation, as shown in Fig. 4 and [14].

D. *Image Processing Algorithm*

The heart of the TIS is the remote tactile image processor. It creates the overlaid tactile image from the thoracoscopic video and tactile sensor data. To accomplish this, the following steps are completed at a rate of 15 Hz:

1. The image from the thoracoscopic video tower is captured and digitized.
2. An image processing algorithm locates the tactile sensor position and orientation in the image plane using colored LEDs located on the head of the probe.
3. The location and area of each tactile sensor element is determined in the image plane.
4. The pressure reading for each element is displayed to the user as a pseudo color overlay.
5. The transparency of previously painted regions is incrementally increased, giving the color map a finite temporal persistence.
6. The composite TIS image is displayed on a monitor visible to the surgeon in the sterile field.

Although there has been progress in marker-less vision-based tool tracking for unmodified laparoscopic tools [15], magnetic tracker-based tool localization [16], and three dimensional ultrasound [17], the requirement for simple, robust, real-time tracking of position and orientation led to a marker-based visual solution. Small surface mount LEDs instead of passive markers were used because of the unpredictable background colors and intensities that exist inside the thoracic cavity. Furthermore, the LEDs blink and the marker-tracking algorithm is based on color change rather than absolute color to limit the noise introduced when the light source creates surfaces as bright and colorful as an LED.

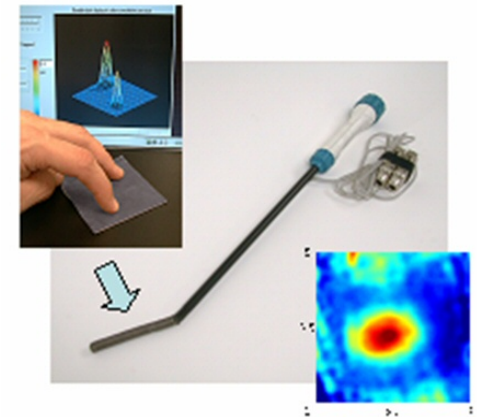

Fig. 3. Integration of capacitance-based sensor array with minimally invasive probe.

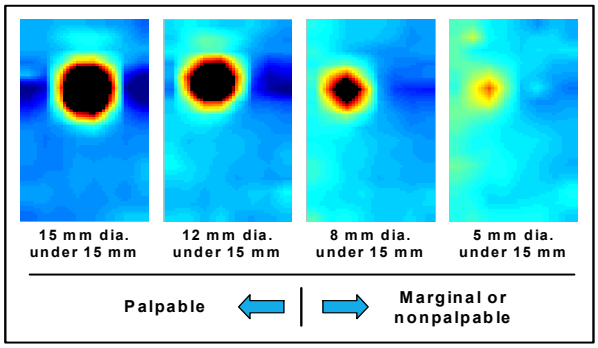

Fig. 4. Recorded image of various lesion sizes as recorded by the SureTouch Visual Mapping System [14].

For this prototype, blue LEDs are placed at the proximal and distal ends of the top of the sensor head. By wiring them in parallel with opposite polarity, they can be controlled with only two traces. The LED blink rate is controlled by the software, so successive captured frames display alternate LEDs.

The program loops through each captured image and compares the blue value of each pixel with that of the pixel on the previous frame. If a pixel's blue value has changed by a threshold amount, that pixel is tagged as a part of the LED marker. Because the code detects positive and negative value changes, it locates both the lit and unlit LED in each frame.

Once the LEDs are located, two-dimensional position and orientation of the sensor area within the image are calculated. Position is indicated by the LED locations. Orientation can be calculated from the angle of the line created by the two LED locations. A scaling factor, proportional to the distance between the camera and the scanning plane, can be calculated from the distance between the LEDs. Fig. 5 shows a diagram of the probe as seen in the captured image.

The Equation (1) is derived using the terminology of Fig. 5. This equation maps the sensor element of row *i*, column *j* to a pixel in image-space. In Equation (1), the symbol *scale* is the ratio of image pixels to real-world millimeters. *Offset* is the distance in mm from point *P* to the first sensor element. k_1 is the distance in mm between rows of sensor elements. k_2 is the distance in mm between columns of sensor elements.

A simple vector sum solution is sufficient for the two-

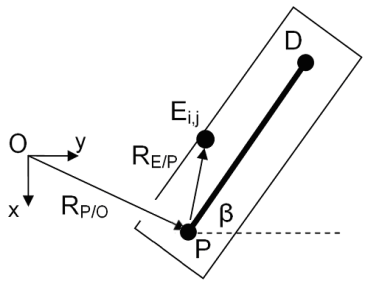

Fig. 5. O is the upper left pixel of the image (row = 0, column = 0). P is the LED at the rear of the head; D is the LED at the tip. β is the angle of the probe head with respect to the y-axis. $E_{i,j}$ is the location of the sensor element in the i-th row, j-th column.

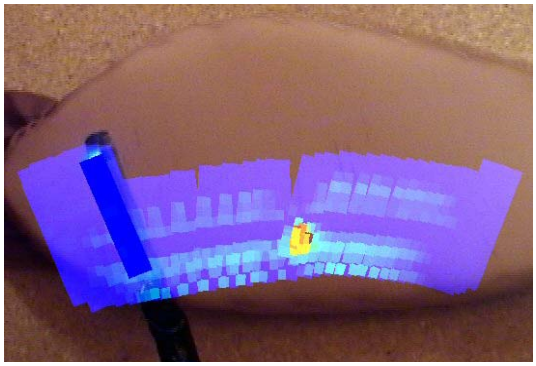

Fig. 6. Overlaid pressure data on the laparoscopic image. The yellow and red indicates a imbedded lump.

dimensional problem. Note that this method performs a Euclidean transform on the sensor data, limiting the overlay to a simple in-plane rectangle. The program plots each sensor element as a different pseudo-color corresponding to the sensed pressure.

$$\vec{E}_{i,j} = \vec{R}_{P/O} + \vec{R}_{E/P}$$

$$\vec{E}_{i,j} = \vec{R}_{P/O} + scale \cdot \left[(offset + k_1 \cdot i) \cdot \begin{pmatrix} \sin\beta \\ \cos\beta \\ 1 \end{pmatrix} + k_2 \cdot (j-1) \cdot \begin{pmatrix} -\cos\beta \\ \sin\beta \\ 1 \end{pmatrix} \right] \quad (1)$$

Fig. 6 shows an example of the color persistence in action. This color data persists on the screen for a few seconds after it is recorded so the user can compare the current data to that of the surrounding area. The concentration of hot colors in the center of the swipe indicates that a hard spot exists in the foam model at that location. To filter the pressure data, several methods are used. First, a baseline is calculated when the system is initialized and is subtracted off of every reading. Second, the average pressure value of all the sensor elements is calculated and subtracted from each element on each frame. These filters tune the system to accentuate a narrow peak in pressure, which is the expected effect of a lung nodule.

III. Validation Experiment

A validation experiment was performed to test the relative performance of the Tactile Imaging System. The goal of the experiment was to determine if and in what ways the system was better than basic instrument palpation with a rigid rod.

A. Inanimate Lung Phantoms

Eight foam lung phantoms with embedded lumps were created for this experiment. To make the phantoms, lung-like shapes were cut from 1 inch foam blocks, and then bisected horizontally. Five beads of sizes 4, 6, 8, 10, and 12 mm were randomly scattered and glued between the halves such that they were not visible through the phantom surface. The pieces were then sewn together, wrapped in hosiery and taped to a wooden block.

A phantom was reviewed by a clinical collaborator, who described it as "a decent model" of a lung and indicated that the nodules' "location and feel are appropriate" for a validation experiment. A typical phantom is visible in Fig. 6.

To further justify the use of the lung phantoms, a force-displacement curve was generated by indenting a phantom with a 19.1 mm spherical indenter actuated by a linear slide with a mounted force gage. The position and force resolution of the device are +/- 0.0075 mm and +/- 0.01 N. Fig. 7 shows the curve as compared to a similar dataset measuring lung tissue generated by Lai-Fook et al. [18]. Though the curves ultimately diverge, the phantoms still emulate lung sufficiently for the purposes of this experiment.

B. Experimental Setup

The validation experiment was set up to loosely imitate actual surgical conditions. The phantom is placed inside a cardboard box that has a large hole in the top and a small hole in the lower front face. A camera imitating the thoracoscope looks down through the top hole and the tool palpates through the front hole. When using this setup, the situation differs from an actual VATS procedure in that the camera views a much larger area and without the perspective distortion caused by a wide-angle view.

Fig. 8 shows the apparatus from the angle of the subject. The subject stands in front of the table, manipulating the tool with his or her right hand while watching the computer monitor. The proctor stands on the far side, views the same image, advances the experiment program with the keyboard, and switches phantoms as needed. The rigid rod used in this experiment, as shown in the bottom of Fig. 8, is a 56 cm long, 5 mm diameter aluminum rod with a rounded end. It is directly comparable to a typical rod used in the operating room for instrument palpation.

C. Experimental Methods

Six unpaid subjects participated in this experiment (5 males, 1 female, mean age 25). None had clinical experience and four had previously used haptic interfaces in a laboratory setting.

To reduce the error attributed to a learning curve, the subjects were first given an example phantom and told to directly palpate it with their hand until they found all the

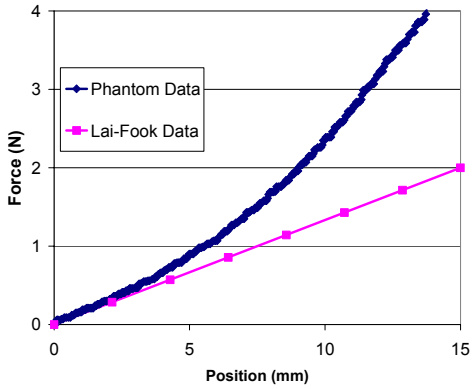

Fig. 7. Force-Displacement data from a lung phantom used in the validation experiment compared to actual lung measured by Lai-Fook [18].

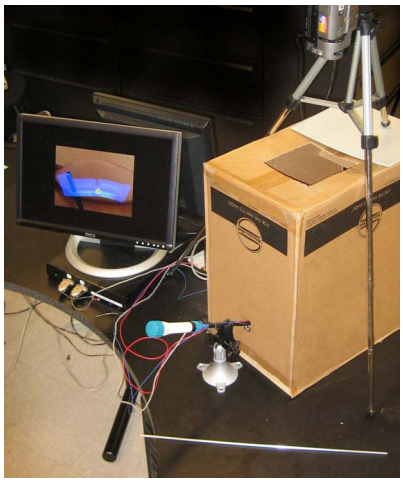

Fig. 8. The experimental setup from the perspective of the subject. The screen image is simulated.

beads. They were then instructed to do the same task with the phantom in the experimental setup. During this experience, the proctor advised the subject in the way to most effectively use the tools. The subject was then told to continue practicing with both tools until he or she was comfortable with and confident in their use.

Before each trial, the subjects were told that the phantom contained five randomly placed beads, one of each size (4, 6, 8, 10, and 12 mm). Each subject then attempted to find all embedded beads in the phantoms. Each subject completed 8 trials, 4 with one tool and then 4 with the other. The tool order (rod or TIS) and phantom number were randomized.

Three experimental parameters were measured: total time taken, the number and size of beads found, and the number of false positives.

D. *Experimental Results*

The experimental results show the Tactile Imaging System is a faster, more accurate method for finding embedded nodules of any size. Completion times are shown in Fig. 9. The error bars indicate one standard deviation in each direction. A two-way ANOVA showed participants performed the task significantly faster with the probe than with the rod [$F(1,36) = 12.06$, $p = 0.001$]. The interaction between experimental conditions and subjects was non-significant ($p > 0.5$), indicating that participants performed similarly across conditions and the results are generalizable to the sample population.

In addition, the subjects were able to locate smaller lumps with greater frequency while using the probe, as seen in Fig. 10. Using the probe, subjects recorded 9 false positives, while they recorded 16 when using the rod.

Exit interviews were performed for each subject. All six subjects complained that they had to exert much more force while using the rod, with five of them having to take breaks or complaining of hand pain. Five subjects also complained about the tiny scanning area of the rod.

After using the probe, four subjects complained that the method for articulating the head was difficult and time consuming and three complained that the signal noise reduced their certainty about lump location.

IV. Discussion

The validation experiment and exit interviews show that the Tactile Imaging System is a superior method for finding embedded lumps in softer, homogeneous structures. On average, subjects were able to locate each nodule much faster with the TIS and were generally able to find smaller lumps.

The validation experiment also showed that the success of the probe depends heavily on the technique of the user. Subject 5 in the experiment never was able to feel fully comfortable using the probe, to the detriment of his or her performance. The subject's method for palpating when using the rod is also of concern. All six subjects found that the best way to find lumps was to push the tip down into the phantom and then move forward while maintaining high force with both hands. This method would cause significant damage to actual lung tissue and be unusable in real life. Therefore, this experiment makes the rod look more accurate than it would be in a real world application.

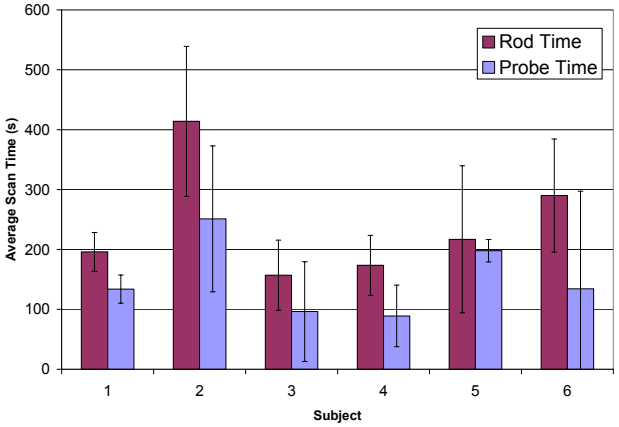

Fig. 9. Time data from the validation experiment. The error bars show one standard deviation in each direction.

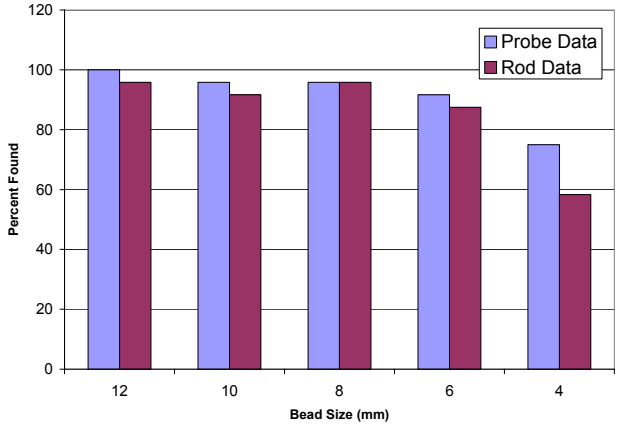

Fig. 10. Percentage found for each bead size.

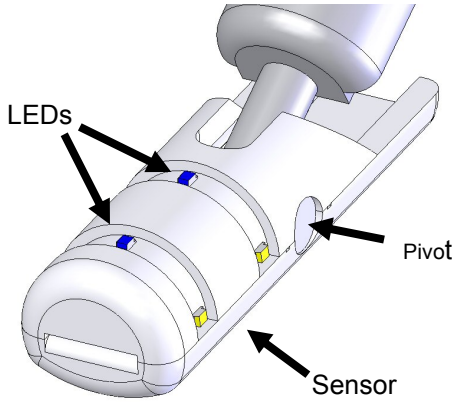

Fig. 11. CAD drawing of the next probe prototype.

The current design of the probe limits the effectiveness of the TIS. First, the sensor should be more sensitive and consequentially combined with a more powerful noise-reduction algorithm. Second, the joint location on the probe complicates the mechanical forces required to achieve a good reading. If a doctor were to apply an axial force on the current probe, the maximum reaction force on the probe head would be at the joint, which is not covered by the sensor. Third, the method of manually articulating the probe joint is difficult and time consuming. Fourth, the two-LED design is only capable of showing in-plane rotation and translation of the probe head.

Fig. 11 is a drawing of a new probe being built to address these concerns. The sensor will be twice as sensitive as the current model. The probe will have a passive joint in the center of the sensor area, so when pressed against a surface, the probe will automatically flatten against it and directly transfer forces. It will also have six LEDs of various colors, giving the image processing software enough data to solve the three dimensional problem. Using this new design, a follow on experiment is planned using thoracic surgeons as subjects and excised lung.

V. Conclusion

Palpation is used extensively in all types of surgery and provides valuable information for diagnosis and control in many surgical tasks. The development of remote palpation technology will allow surgeons to regain some of the tactile information lost during minimally invasive surgery. Localization of pulmonary nodules is our initial target application, but other localization tasks could also be enhanced. Artery localization, bowel or liver palpation, and determination of tissue stiffness for needle placement all stand to benefit from tactile imaging technology.

Robotic surgery could also be enhanced by incorporating remote palpation sensors. A lack of haptic feedback is often reported as a major limitation to current robotic devices. Remote palpation during minimally invasive surgery can reach a new level by combining the dexterity and precision of a surgical robot with useful information collected with distributed pressure sensing tactile arrays.

Acknowledgment

Mike G for his help with the experimental setup and Steve C for assisting with the statistical analysis.

References

[1] Jemal A, Murray T, Ward E, et al. Cancer statistics, 2005. CA Cancer J Clin 2005;55:10-30. [Erratum, CA Cancer J Clin 2005;55:259.]

[2] Ries LAG, Harkins D, Krapcho M, Mariotto A, Miller BA, Feuer EJ, Clegg L, Eisner MP, Horner MJ, Howlader N, Hayat M, Hankey BF, Edwards BK (eds). SEER Cancer Statistics Review, 1975-2003, National Cancer Institute. Bethesda, MD, http://seer.cancer.gov/csr/1975_2003/, based on November 2005 SEER data submission, posted to the SEER web site 2006.

[3] Etzioni, R., Urban, N., Ramsey, S., McIntosh, M., Schwartz, S., Ried, B., Radich, J., Anderson, G., and Hartwell, L. "The case for early detection." *Nature Rev. Cancer* 3**,** 243–252 2003.

[4] Lillington GA. "Management of solitary pulmonary nodules." *Dis Mon* 1991;37(5):271-318

[5] Munden RF, Pugatch R, Liptay MJ, Sugarbaker DJ, Le LU. "Small pulmonary lesions detected at CT: clinical importance." *Radiology* 1997;202:105–110

[6] Mack MJ, Shennib H, Lanreneau RJ, and Hazelrigg SR. "Techniques for localizing of pulmonary nodules for thoracoscopic resection." *J Thoracic Endoscopic Surg Allied Technol* 1993;106(3):550-553

[7] Plunket MB, Peterson MS, Landreneau RJ, Ferson PF, Posner MC. "Peripheral pulmonary nodules: preoperative percutaneous needle localization with CT guidance." *Radiology* 1992;185:274-6

[8] Li H, Boiselle PM, Shepard JO, Trotman-Dickenson B, McLoud TC. "Diagnostic accuracy and safety of CT-guided percutaneous needle aspiration biopsy of the lung: comparison of small and large pulmonary nodules." *AJR* 1996;167:105–109

[9] Santambrogio R, Montorsi M, Bianchi P, Mantovani A, Ghelma F, Mezzetti M. "Intraoperative ultrasound during thoracoscopic procedures for solitary pulmonary nodules." *Ann Thorac Surg* 1999 Jul;68(1):218-22

[10] Kerviler E. "Limitation of intraoperative sonography for the localization of pulmonary nodules during thoracoscopy." *AJR* 1998; 170:214-215

[11] Kawahara T, Toya C, Tanaka N, Kaneko M, Miyata Y, Okajima M, and Asahara T. "Non-Contact Impedance Imager with Phase Differentiator," Proc. of the 1st IEEE/RAS-EMBS Int. Conf. on Biomedical Robotics and Biomechatronics, #159, 2006.

[12] Peine WJ. "Remote palpation instruments for minimally invasive surgery," Ph.D. Thesis, Harvard University, Division of Engineering and Applied Sciences 1998

[13] Pawluk DTV, Son JS, Wellman PS, Peine WJ, and Howe RD. "A Distributed Pressure Sensor for Biomechanical Measurements," *ASME Journal of Biomechanical Engineering* 102(2):302-305, April 1998.

[14] Kearney TJ, Airapetian S, and Sarvazyan A. "Tactile breast imaging to increase the sensitivity of breast examination." *J Clin Oncol* 2004; 22supp:103

[15] Voros S, Orvain E, Long JA, Cinquin P. "Automatic Detection of Instruments in Laparoscopic Images: a First Step towards High Level Command of Robotized Endoscopic Holders." Proceedings of BioRob 2006.

[16] Wellman PS. Tactile Imaging. Ph. D. Thesis, Harvard University, Division of Engineering and Applied Sciences 1999

[17] Novotny PM, Stoll JA, Vasilyev NV, Del Nido PJ, Dupont PE, and Howe RD. "GPU Based Real-time Instrument Tracking with Three Dimensional Ultrasound. Medical Image Computing and Computer-Assisted Intervention" – MICCAI, 2006.

[18] Lai-Fook SJ, Wilson TA, Hyatt RE, and Rodarte JR, 1976. "Elastic Constants of Inflated Lobes of Dog Lungs," *J. Applied Physiology*, 40:508-513